Structural and magnetic properties of Fe_4 clusters confined in carbon nanotubes

2007 J. Phys.: Condens. Matter 19 466203

(http://iopscience.iop.org/0953-8984/19/46/466203)

IOP PUBLISHING JOURNAL OF PHYSICS: CONDENSED MATTER

J. Phys.: Condens. Matter **19** (2007) 466203 (13pp) doi:10.1088/0953-8984/19/46/466203

Structural and magnetic properties of Fe_4 clusters confined in carbon nanotubes

Shijun Yuan[1], **Yong Kong**[2], **Fusheng Wen**[1] **and Fashen Li**[1]

[1] Key Lab on Magnetism and Magnetic Materials of the Ministry of Education, Lanzhou University, Lanzhou 730000, People's Republic of China
[2] Max-Planck-Institut für Metallforschung, Heisenbergstrasse 3, Stuttgart 70569, Germany

E-mail: y.kong@mf.mpg.de and lifs@lzu.edu.cn

Received 20 April 2007, in final form 3 October 2007
Published 23 October 2007
Online at stacks.iop.org/JPhysCM/19/466203

Abstract

First-principles calculations based on density-functional theory are performed to study small iron clusters (Fe_4) encapsulated in single-walled carbon nanotubes (SWCNTs). We calculate the total energy and electronic structure of confined Fe_4–SWCNT systems, and examine confining effects of the SWCNTs on equilibrium structure and magnetic properties of Fe_4. Compared with isolated free Fe_4, the 'templating' effect of SWCNTs due to strong Fe–C interaction distorts the structure of the confined Fe_4 from a D_{2d} geometry to a low-symmetry tetrahedral or a planar chain structure, depending on the diameter of the SWCNTs. While strong Fe–C sp hybridization suppresses the sp spin polarization of Fe atoms, the charge transfer from sp to Fe 3d in the confined structures was found to reduce the 3d magnetic moment of Fe atoms. Our study suggests that the carbon nanotube and its analogues can be further exploited as a template or regulator for the design of nanoscale magnets with controllable structure and properties.

1. Introduction

Carbon nanotubes (CNTs) have played a significant role in emerging nanoscience and nanotechnology [1]. Owing to their unique quasi-one-dimensional atomic structure and superb mechanical, physical and chemical properties, CNTs are becoming important building blocks for applications in nanoelectronics [2–4] and miniature electromechanical devices [5]. In the past few years, there has been considerable interest in filling CNTs with various materials to explore interesting structures and property-tuning functions [6–9]. The hollow cavity of a nanotube can serve as an ideal storage medium for atoms and small molecules [7–9], as well as a nanometer-scale capsule for chemical reactions [10]. It is well known that chemical instability has limited the applications of small-sized clusters at ambient conditions. Acting as protective shells, metal-filled CNTs improve the stability of the encapsulated metal clusters,

and are expected to have diverse applications in nanoscale devices. In particular, CNTs filled with magnetic species, such as iron [11], cobalt [12], and iron oxide [13], can be considered as potential candidates for use in spin-polarized nanodevices or magnetic storage materials as proposed by previous publications [13–16].

On the other hand, nanotube production involves widespread use of transition metal (TM) catalysts such as Ni, Co, or Fe. Despite purification, there are catalytic particles remaining on the tip ends or the tube wall of CNTs, which may affect the properties of CNTs and consequently the performance of CNT-based devices [17]. Although the influence of such residual metal catalysts cannot be ruled out in most cases, study of the interaction of TM atoms with nanotubes—particularly the bonding details of the metal atoms with carbon in CNTs—should enable us to understand the effects of metallic catalyst residues.

As a typical magnetic TM and frequently used catalyst in the growth process of CNTs, Fe-filled CNTs have been therefore the subject of many theoretical [18–20] and experimental [21, 22] studies. Fagan *et al* [18] studied the interaction of an iron atom on an (8, 0) semiconducting zigzag nanotube by first-principles calculations. The most stable configuration was found to be a hole site outside of the nanotube. The magnetic moment (3.90 μ_B) for the outside configuration is higher than the inside (2.36 μ_B) due to stronger hybridization and a confining effect inside. Kang *et al* [19] and Weissmann *et al* [20] theoretically studied CNT-encapsulating Fe nanowires with a bulk structure of bcc and hcp, respectively. By comparing with the free-standing wires, they examined the effect of interactions between the Fe and C atoms on the magnetic properties of Fe nanowires in single-walled CNTs (SWCNTs) and found that the magnetic moments of thin nanowires are similar to those for the free-standing nanowires, while they are greatly reduced for thicker nanowires owing to stronger interaction between under-coordinated Fe atoms and nanotubes. Using cross-sectional high-resolution transmission electron microscopy and spatially resolved electron energy loss spectroscopy, Jin-Phillipp and Rühle [21] observed a semicoherent CNT/Fe interface with local lattice mismatch in Fe-filled multi-walled CNTs, and experimentally proved an interfacial bonding between the CNT wall and Fe.

In order to advance the CNT–TM interaction, it might be better to consider SWCNT encapsulating a small TM cluster, rather than a single atom or nanowire with predefined bulk structures. With the partially filled cluster it is more convenient to investigate the carbon–TM bonding details and to study the confining effect of CNT on the structure and properties of filled metals. The understanding of the inhomogeneous 'local' CNT–TM interaction may also enable us to explore the influence of the filled metals on CNT properties, which could give insight into the interaction of CNT with metallic catalyst residues.

In this paper, we present the results of first-principles calculations on a small iron cluster Fe_4 confined in (5, 5), (6, 6) and (8, 0) CNTs. We calculate total energies and electronic structures of the Fe_4–SWCNT systems, and focus on the effects of Fe–C interaction on equilibrium structure, electronic and magnetic properties of the confined Fe_4 cluster. Our results demonstrate a large confining effect of the CNT on the Fe_4 cluster owing to strong Fe–C interaction, which dramatically distorts the geometry of the Fe_4 and results in a prominent change in electronic structure and magnetic moments. In the following sections, we first introduce the computational method and some parameters used in all our calculations, and then present our main results and the discussion. Finally, an overall conclusion is included.

2. Calculation details

All the calculations are performed with a DFT-based spin-polarized first-principles approach using pseudopotentials and localized numerical orbitals, as implemented in the SIESTA

package [23]. The core electrons were represented by norm-conserving Troullier–Martins pseudopotentials [24] in the fully nonlocal Kleinman–Bylander form [25], which are generated by relativistic atomic calculations and included nonlinear core corrections to account for the significant overlap of the core charge with 3d orbitals. The valence orbitals were expanded using linear combination of numerical pseudoatomic orbitals [26]. In our calculations, we use a standard double-ζ basis set with polarization functions (DZP) for carbon and an optimized DZP basis set for iron atoms [27]. We use the generalized gradient approximation (GGA) as proposed by Perdew–Burke–Ernzerhof [28] for exchange and correlation energy, which is based on the suggestion by Hobbs *et al* that the gradient corrections are absolutely essential in predicting the correct magnetic ground states of small clusters [29]. A cut-off of 400 Ryd for the grid integration was used to represent charge density in all the calculations, for which the structure and electronic energies are fully converged. In the present paper, we have not included the noncollinear effect owing to the size of the Fe_4–SWCNT system and our computational limits.

We consider three model systems in the present study: an Fe_4 cluster was confined in a single-walled (5, 5), (6, 6) and (8, 0) CNT, respectively. In the calculations we use periodic boundary conditions and a hexagonal supercell approximation with a lateral separation of 25 Å between tube centers, which is large enough to prevent any interaction of the tubes with their periodic images. A supercell consisted of four Fe atoms and seven armchair CNT layers containing 140 carbon atoms for a (5, 5) and 168 carbon atoms for a (6, 6) tube, or four zigzag CNT layers with 128 carbon atoms in an (8, 0) tube. The resulting length of the supercell was about 17.40 Å for two metallic tubes, and 17.22 Å for the semiconducting tube, which should be enough to make sure that the Fe clusters in neighboring cells do not interact with each other.

In order to find out the equilibrium structure for the CNT-confining Fe_4 cluster, we set up various initial configurations where the Fe_4 was randomly placed inside the tubes, and optimized their structures by relaxing all the atomic coordinates. The structure optimization is performed by the conjugated-gradient algorithm until the residual force is less than 0.04 eV $Å^{-1}$. To reduce computational costs, in the structure optimization only a single k point was used for Brillouin-zone (BZ) integration. Given a fully relaxed configuration, a denser $1 \times 1 \times 14$ k-grid was used to calculate total energy, electronic structure and magnetic moments.

To test the current setup for calculations, as a reference, we study single-walled (5, 5), (6, 6) and (8, 0) CNTs and an isolated free Fe_4 cluster at first. For both (n, n) SWCNTs we get an axial unit length of 2.48 Å for the armchair CNTs, corresponding to a mean C–C bond length of 1.435 Å, which is about 1% larger than the experimental 1.418 Å. Our result is reasonable when considering the general overestimation of equilibrium bond length caused by the GGA. For the isolated free Fe_4 a ferromagnetic D_{2d} structure with a total magnetic moment of 14.0 μ_B was obtained, which agrees very well with the previous result [29]. The optimized structures for the free Fe_4 cluster and pristine (5, 5), (6, 6) and (8, 0) CNTs are further adopted into initial configurations for structure relaxation of the confined Fe_4 + CNT systems.

3. Results and discussion

Before discussing the Fe_4 cluster confined in CNT, we first consider an isolated free Fe_4 cluster. Small-sized Fe clusters have been extensively studied by experiments [30–33] and theoretical calculations [29, 34–36]. Both the local-density-approximation (LDA) and the GGA predicted a ferromagnetic ground state with a tetrahedral structure. Compared with the LDA results, however, the GGA calculations predicted not only a larger total magnetic moment (14 μ_B) but also a distorted tetrahedral structure instead of a regular tetrahedron with T_d symmetry [29].

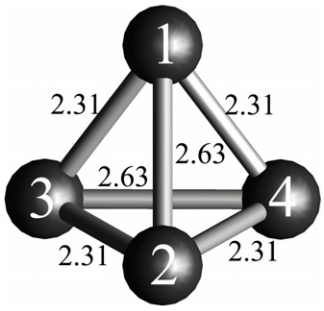

Figure 1. Optimized configuration for an isolated Fe_4 cluster. In the D_{2d} structure two opposite, mutually perpendicular bonds are 2.63 Å and the remaining four 2.31 Å.

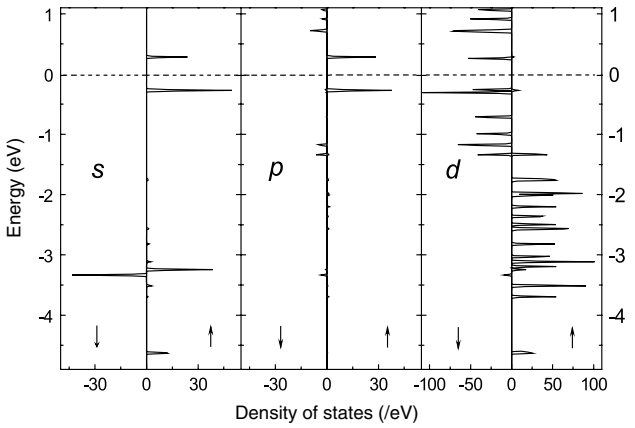

Figure 2. s-, p- and d-projected DOS calculated for the isolated Fe_4 cluster with the D_{2d} structure. The Fermi level is set to 0.0 eV. The arrows indicate majority (up) and minority (down) spins.

Starting from a free Fe_4 with regular tetrahedral structure, we get similar results from our calculations, which predicted a ferromagnetic ground state with a distorted tetrahedral structure (D_{2d} symmetry), as shown in figure 1. Compared to the regular tetrahedron, in the D_{2d} structure two opposite, mutually perpendicular Fe–Fe bonds are considerably stretched (2.63 Å), whereas the remaining four edges are shortened by 0.32 Å, resulting in four congruent isosceles (non-equilateral) triangles. According to the Mulliken population analysis, all four Fe atoms have approximately the same electronic configuration, $3d^{6.7}4(sp)^{1.3}$. In figure 2 we show the orbital-projected density of states (DOS) calculated for the D_{2d} Fe_4. All the s, p and d DOSs are featured by atom-like discrete peaks. The 3d states with majority spins are almost fully occupied, resulting in a strong spin polarization. Prominent hybridization between sp and d electrons was observed near the Fermi level and in the region between -4.0 and -3.0 eV. For the $D_{2d}Fe_4$ we obtain an atomic magnetic moment of 3.5 μ_B for each Fe atom, to which the 3d spin polarization contributes 3.13 μ_B and the 4s, 4p electrons give a contribution of 0.21 and 0.16 μ_B in addition.

Depending on the initial position and orientation of the D_{2d} Fe_4, the structure optimizations for the Fe_4 confined in (5, 5) CNTs have two stable structures converged, labeled as (5, 5)T1 and (5, 5)T2, which are illustrated in figure 3 with both top and side views. For the Fe_4 clusters confined in (6, 6) CNTs, three stable Fe_4 configurations shown in figure 4 were obtained from

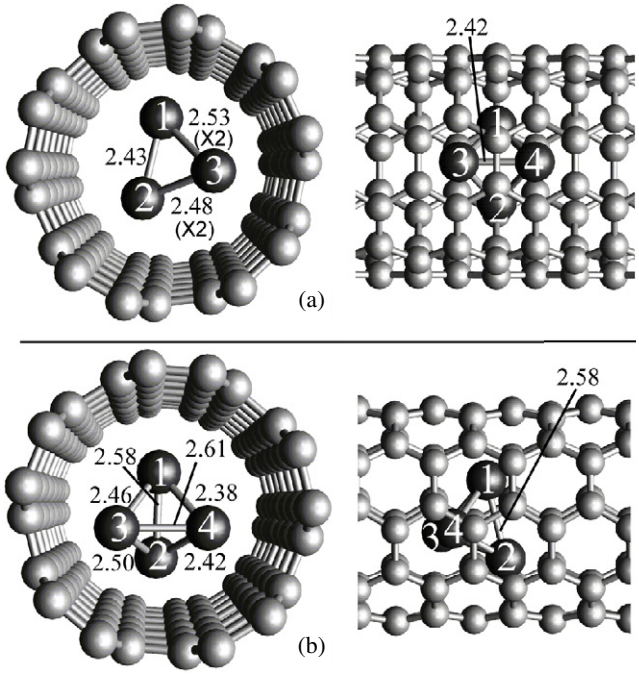

Figure 3. Top and side views of the optimized (5, 5)T1 (a) and (5, 5)T2 (b) structures for a Fe_4 cluster confined in a (5, 5) CNT. Gray and black balls represent carbon and iron atoms, respectively. Four iron atoms are labeled by the numbers 1, 2, 3 and 4. Also shown in the figures are the Fe–Fe bond lengths (unit: Å).

Table 1. Optimized structures and properties of the CNT-confining Fe_4 clusters. (5, 5)T1 (T2), (6, 6)T1 (T2, CH) and (8, 0)T denote the optimized Fe_4 configurations in (5, 5), (6, 6) and (8, 0) CNTs, respectively. $\overline{d}_{Fe-C}$ and $\overline{d}_{Fe-Fe}$ represent the averaged Fe–C and Fe–Fe distances. M is the total magnetic moment of the Fe_4 clusters and E_B the binding energy between Fe_4 and CNT. The results for free Fe_4 were also listed for comparison.

	Free Fe_4	(5, 5)T1	(5, 5)T2	(6, 6)T1	(6, 6)T2	(6, 6)CH	(8, 0)T
Symmetry	D_{2d}	C_s	—	C_2	C_s	—	—
$\overline{d}_{Fe1-C}$ (Å)	—	2.50	2.49	2.42	2.22	2.35	2.19
$\overline{d}_{Fe2-C}$ (Å)	—	2.39	2.39	2.38	2.17	2.28	2.26
$\overline{d}_{Fe3-C}$ (Å)	—	2.45	2.39	2.42	2.22	2.28	2.28
$\overline{d}_{Fe4-C}$ (Å)	—	2.45	2.31	2.38	—	2.34	2.35
$\overline{d}_{Fe-Fe}$ (Å)	2.42	2.48	2.43	2.43	2.39	2.33	2.45
M (μ_B)	14.0	11.5	11.6	11.5	11.0	11.4	11.3
E_B (eV)	—	4.57	4.85	3.47	3.61	2.58	4.31

the structure relaxations. Two optimized tetrahedral structures were labeled as (6, 6)T1 and (6, 6)T2, and the third one with a planar chain-like structure as (6, 6)CH. The averaged Fe–Fe and Fe–C bond lengths for the three structures were summarized in table 1.

For further understanding of the confined Fe_4 clusters, we calculate the binding energies of the confined Fe_4 + CNT systems by subtracting the total energy calculated for the relaxed

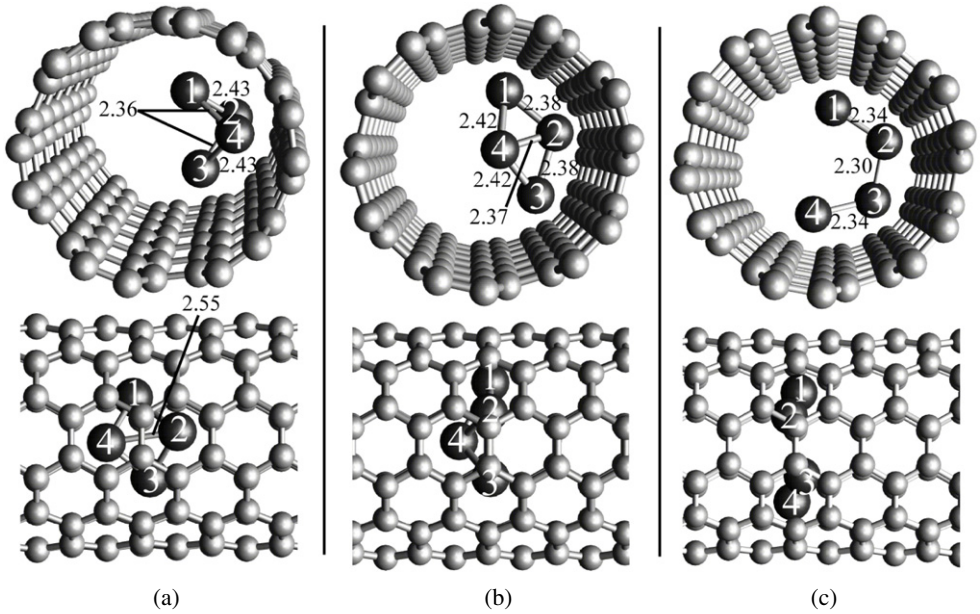

Figure 4. Top and side views of the optimized tetrahedral ((6, 6)T1 (a) and (6, 6)T2 (b)) and chain ((6, 6)CH (c)) structures for an Fe_4 cluster confined in a (6, 6) CNT. Gray and black balls represent carbon and iron atoms, respectively. Four iron atoms are labeled by the numbers 1, 2, 3 and 4. The Fe–Fe bond lengths are also shown in the figures (unit: Å).

$Fe_4 + CNT$ structures from the sum of the total energies for isolated free Fe_4 and CNTs, i.e. through the expression

$$E_B = E_{CNT} + E_{Fe_4} - E_{Fe_4+CNT},$$

where E_{CNT} and E_{Fe_4} are the total energies for the pristine CNT and isolated free Fe_4 cluster shown in figure 1 and E_{Fe_4+CNT} the total energy for the equilibrium structures of the confined $Fe_4 + CNT$ systems. The calculated E_B values for (5, 5)T1, (5, 5)T2, (6, 6)T1, (6, 6)T2 and (6, 6)CH structures are listed in table 1. We find that in the (5, 5) tube the low-symmetry (5, 5)T2 is more stable than the C_s (5, 5)T1 structure, and the (6, 6)T2 with the C_s symmetry is the most stable structure in the (6, 6) tube. Both the tetrahedral $Fe_4 + (5, 5)$ structures have the binding energy about 1 eV higher than two tetrahedral $Fe_4 + (6, 6)$ structures and even about 2 eV higher than the chain structure (6, 6)CH, despite stronger Fe–C interaction in all three $Fe_4 + (6, 6)$ structures. The lower binding energies for $Fe_4 + (6, 6)$ structures should be mainly assigned to the increase in the E_{Fe_4+CNT} caused by strongly distorted Fe_4 structures in the (6, 6) tube, particularly for the (6, 6)CH structure, in which the distorted Fe_4 forms only three Fe–Fe bonds.

The (5, 5)T1 Fe_4 cluster that shapes an irregular tetrahedral structure with C_s symmetry has two pairs of Fe–Fe bonds with equal length: the Fe1–Fe3 and Fe1–Fe4 bonds with a length of 2.53 Å and the Fe2–Fe3 and Fe2–Fe4 with a length of 2.48 Å, which form two unequal isosceles triangles with the Fe1–Fe2 bond (2.43 Å) as a common base. In contrast, all the Fe–Fe bonds in the (5, 5)T2 have different lengths, resulting in no non-trivial symmetrical operation in the structure. Compared to the T1 structure, the Fe1–Fe2 and Fe3–Fe4 bonds in the T2 cluster are dramatically stretched by about 0.15 and 0.2 Å, and the Fe1–Fe4 bond is shortened by 0.15 Å. Rotating the T1 structure around the Fe1–Fe2 bond by 90°, the T2 structure could be then

derived from the T1 by stretching the Fe1–Fe2 and Fe3–Fe4 bonds parallel and perpendicular to the CNT axial direction respectively.

Analyzing the positions of individual Fe atoms in the (5, 5) CNT, we find that in the T1 structure the Fe1 atom is almost sitting on top of one C atom whereas all the other three Fe atoms are approximately positioned on top of C–C hexagonal centers. The Fe3 and the Fe4 are arranged along the axial direction of the CNT with a distance of 2.42 Å, which is slightly smaller than 2.48 Å, the axial unit length of the armchair CNT. For the Fe atoms in the T2 structure only Fe2 and Fe3 are on top of two hexagonal centers. The Fe1 and the Fe4 also occupy positions on the top of C–C hexagons but with an obvious deviation to the top of one C atom and the bridge site of C–C bond, respectively. For more details of the structures of the confined Fe_4 clusters, we list the averaged Fe–C and Fe–Fe bond length, $\overline{d}_{Fe-C}$ and $\overline{d}_{Fe-Fe}$, in table 1. The $\overline{d}_{Fe-Fe}$ and all the $\overline{d}_{Fe-C}$ in the T2 are smaller than those in the T1 structure, suggesting that the Fe–Fe and the Fe–C interactions could be stronger in the confined T2 Fe_4.

The Fe_4 with the (6, 6)T1 structure exhibits the C_2 symmetry and has two pairs of Fe–Fe bonds with equal bond lengths: the Fe1–Fe2 and Fe3–Fe4 bonds with a length of 2.43 Å and the Fe1–Fe4 and Fe2–Fe3 bonds with a length of 2.36 Å, which form two pairs of isomorphic scalene triangles. In the structure Fe1 and Fe3 atoms sit on the bridge sites of C–C bonds perpendicular to the tube axis with an equal $\overline{d}_{Fe-C}$ of 2.42 Å. Fe2 and Fe4 atoms with a distance of 2.55 Å, which is slightly bigger than the axial unit length 2.48 Å, are positioned approximately on the top of C–C hexagonal centers with the same $\overline{d}_{Fe-C}$ of 2.38 Å. The tetrahedral (6, 6)T2 structure also has two pairs of Fe–Fe bonds with equal bond lengths: the Fe1–Fe2 and Fe2–Fe3 bonds and the Fe1–Fe4 and Fe3–Fe4 bonds with lengths of 2.38 Å and 2.42 Å respectively, exhibiting the same C_s symmetry as the (5, 5)T1 structure. Distinct from the (5, 5)T1 structure, the Fe1–Fe3 bond in the (6, 6)T2, being perpendicular to the common base (Fe2–Fe4 bond) of the two unequal isosceles triangles formed by the two pairs of equal-length Fe–Fe bonds, is destroyed by dramatically stretching (to about 4 Å), which makes the (6, 6)T2 Fe_4 more like a board. Compared to the (6, 6)T1, the Fe4 atom in the T2 structure is shifted towards the tube center, by which the Fe2–Fe4 bond is shortened by 0.18 Å and no bond between the Fe4 and C atoms could be formed any more. Moreover, the Fe1 and the Fe3 are moved from the bridge sites in the T1 structure to the top of C–C hexagonal centers with the same $\overline{d}_{Fe-C}$ of 2.22 Å, which is much smaller than the $\overline{d}_{Fe-C}$ in the (6, 6)T1 structure. Together with the Fe2 ($\overline{d}_{Fe3-C} = 2.17$ Å), all three Fe atoms sitting on top of C–C hexagonal centers form a plane perpendicular to the tube axis. In contrast to T1 and T2, the (6, 6)CH structure exhibits a planar chain-like structure with all four Fe atoms sitting approximately on the top of carbon hexagonal centers from a single CNT layer. The (6, 6)CH structure can be viewed as a derivative of the (6, 6)T2 where the Fe4 is shifted from the tube center to the top site of a C–C hexagon by destroying the Fe–Fe bond between Fe4 and the other three Fe atoms. Therefore there exist only three Fe–Fe bonds in the chain structure, as shown in figure 4(c). Compared to the Fe_4 confined in the (5, 5) tube, the three Fe_4 structures in (6, 6) bind to the tube with shorter Fe–C bonds, implying stronger Fe–C interactions in Fe_4 + (6, 6) structures.

There exist two kinds of periodic potential inside the CNT. One is axial, with $\sqrt{3}d_{C-C}$ (d_{C-C} denotes the C–C bond length) as unit length (2.48 Å from present calculations) for all armchair tubes, and another is circumferential, the unit length of which depends on the curvature of the tube. For CNTs with very big diameter, which are more like a graphite sheets, the unit length of the circumferential potential is similar to the axial one. For small CNTs like the (5, 5) tube, the circumferential C–C network is compacted to a small ring. Both the axial and circumferential potentials should have an effect on the Fe_4 cluster inside the tubes. On the other hand, the absorption of the Fe_4 to the tube wall also affects the C–C bonds around the Fe atom, resulting in the distortion of the C–C network. For example, the length of the C–C bond

between carbon atoms binding to Fe is slightly longer than that between carbon atoms without Fe bound, which implies the adsorptive Fe atoms weaken the C–C bonds. The equilibrium structure of the Fe_4 cluster confined in CNTs should therefore be a consequence of balancing all the effects. Since the elongation of C–C bonds due to the binding of the Fe_4 cluster is very small, only 0.01–0.02 Å from our calculations, the competitive Fe–Fe and Fe–C interactions in the confined Fe_4 + CNT systems may dominate the final structure of the Fe_4 clusters.

In the (6, 6)T2 structure there is stronger Fe–C interaction than in (6, 6)T1 due to the shortest Fe–C bonds. Moreover, its tetrahedral structure with shorter Fe–Fe bonds produces the strongest Fe–Fe interaction among the three structures in the (6, 6) tube. Though the (6, 6)CH structure has the strongest Fe–C bonds (all four Fe atoms take sites on top of C–C hexagonal centers), the strongly distorted Fe_4 structure results in the lowest binding energy due to the weakest Fe–Fe bonding. This implies the Fe–Fe binding is slightly stronger than Fe–C binding in the (6, 6) tube. For two Fe_4 +(5, 5) structures, shorter Fe–C and Fe–Fe bonds enhance both the Fe–C and Fe–Fe interactions in T2 and make it more stable than the T1 structure. It is suggested that a more stable Fe_4 structure inside the CNT should have stronger Fe–Fe and Fe–C bonds at the same time.

Having analyzed various structures of the Fe_4 confined in (5, 5) and (6, 6) tubes, as discussed above, we propose the most favorable absorption site of Fe atoms in the armchair CNTs should be the top site of a C–C hexagonal center. In fact, we have revisited the case where a single Fe atom is absorbed inside a CNT as studied by Fagan *et al* [18], and confirmed the optimized configuration of the Fe atom just sitting on top of the center of a C–C hexagon. From the energetic point of view, all the Fe atoms should occupy the preferred site, provided that the spacing between two such sites can satisfy the length requirement for a reasonable Fe–Fe bond. Otherwise, the Fe atoms could be shifted to other sites like the bridge site of a C–C bond or the top site on a C atom in order to keep the Fe–Fe bonds in existence. With this understanding, the CNT in the confined Fe_4 + CNT system acts mostly like a template, with which the Fe atoms are preferably placed on their favorable sites. It is the competition between the 'templating' effect of CNT and the Fe–Fe interaction that changes the structure of the Fe_4 cluster, resulting in various distorted Fe_4 structures confined in the CNTs. The (6, 6) tube has bigger diameter and smaller curvature than the (5, 5) tube; the confined Fe_4 cluster is more flexible to move in the tube in order that the competition can be better balanced, resulting in more variations in structure. We obtain therefore the compacted tetrahedral Fe_4 structures like (5, 5)T1 and (5, 5)T2 in the (5, 5) tube whereas the extended board-like (6, 6)T2 or chain-like (6, 6)CH in the (6, 6) tube.

We predict ferromagnetic ground states for all the stable Fe_4 structures in (5, 5), (6, 6) and (8, 0) CNTs. The total magnetic moments M calculated for the confined Fe_4 were listed in table 1. Compared to the free Fe_4, the dramatically reduced M for all five confined Fe_4 clusters demonstrated a remarkable confining effect of the CNT on the magnetic properties of the Fe_4, resulting from strong Fe–C interactions in the confined geometry, which is in agreement with previous studies [18–20] on the iron systems confined in CNTs.

To explore the confining effect of the CNT on electronic structures and magnetic properties of the Fe_4 cluster, we summarize the atomic charges and magnetic moments of the Fe_4 in (5, 5) (6, 6) and (8, 0) CNTs together with those of free Fe_4 in table 2. Compared to the free Fe_4, the confinement of CNTs results in a remarkable reduction of the μ_{Fe} from 3.50 to about 2.7–3.0 μ_B, depending on the positions of the Fe atoms in the CNTs. For Fe_4 confined in a (5, 5) tube, most of the Fe atoms have magnetic moments around 2.9 μ_B with the exception of Fe2 (2.72 μ_B) in (5, 5)T1. Considering that the Fe2 is positioned on top of a C–C hexagonal center and has the shortest Fe–C bond length in the structure, its smaller μ_{Fe} could arise from the stronger interaction with carbon than other Fe atoms. In the (6, 6) tube, the μ_{Fe} exhibits quite a

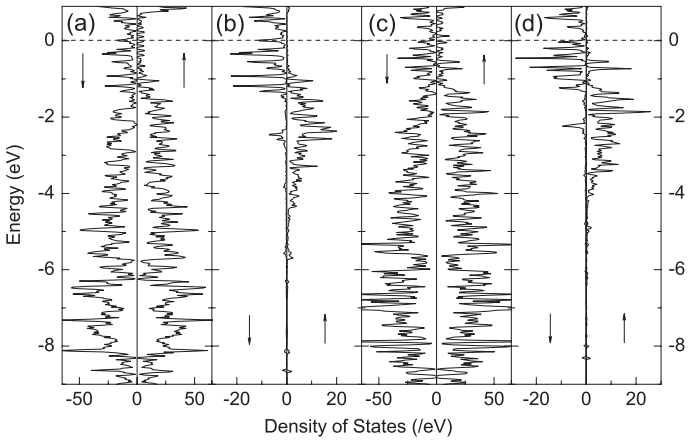

Figure 5. Spin-polarized DOS calculated for the Fe_4 + CNT systems with (5, 5)T2 ((a), (b)) and (6, 6)T2 ((c), (d)) structures. Shown in panels (a) and (c) are the total DOS, and in (b) and (d) the partial DOS projected for the confined Fe_4 clusters. The Fermi energy is set to 0.0 eV. The arrows indicate majority (up) and minority (down) spins.

Table 2. Electronic charges and magnetic moments of the Fe atoms in Fe_4 clusters. (5, 5)T1 (T2), (6, 6)T1 (T2, CH) and (8, 0)T represent the optimized Fe_4 structures in (5, 5), (6, 6) and (8, 0) CNTs. The Fe1, Fe2, Fe3 and Fe4 atoms are labeled the same as in figures 3, 4 and 7. (Notice that the data listed below were obtained directly from Mulliken population analysis, and may contain certain errors owing to the method limits.)

	Fe1		Fe2		Fe3		Fe4	
	q (e)	μ_{Fe} (μ_B)	q (e)	μ_{Fe} (μ_B)	q (e)	μ_{Fe} (μ_B)	q (e)	μ_{Fe} (μ_B)
Free Fe_4	8.00	3.50	8.00	3.50	8.00	3.50	8.00	3.50
(5, 5)T1	8.00	2.93	8.04	2.72	8.03	2.94	8.03	2.93
(5, 5)T2	8.03	2.84	8.01	2.90	8.03	2.97	8.03	2.92
(6, 6)T1	7.96	3.01	8.02	2.76	7.96	3.01	8.02	2.76
(6, 6)T2	8.03	2.79	8.11	2.22	8.03	2.78	7.94	3.18
(6, 6)CH	7.98	3.06	8.06	2.62	8.06	2.63	7.99	3.07
(8, 0)T	8.07	2.74	8.05	2.74	8.05	2.92	8.01	3.10

big fluctuation due to strongly distorted Fe_4 structures. In particular, the Fe2 and the Fe4 atoms in the (6, 6)T2 structure possess the smallest (2.22 μ_B) and the largest (3.18 μ_B) moments among all the structures studied here, respectively. Noticing that the Fe2 sitting on top of the C–C hexagonal center binds to the C atoms by the shortest length of 2.17 Å whereas the Fe4 near the tube center has no direct binding to C atoms, it is the Fe–C interaction that reduces the μ_{Fe} at Fe2.

In figure 5 we plot the DOS calculated for the two most stable Fe_4 + CNT systems, (5, 5)T2 and (6, 6)T2, and the partial DOS projected for Fe_4 in the structures. Distinct from the DOS shown in figure 2, the DOSs for both confined Fe_4 demonstrate an extended, continuous structure with broadened peaks, indicating strong hybridization between Fe and C states. The Fe–C hybridization occurs mainly in the energy region from the Fermi level down to about −4 eV, and results in change transfer between Fe and C atoms. As indicated in table 2, most of the Fe atoms positioning on top of C–C hexagonal centers, which strongly hybridize

Table 3. Partial charges q (unit: e) and orbital-projected spin polarizations μ_{Fe} (unit: μ_B) of the Fe iron atoms in confined Fe_4 clusters. The Fe1, Fe2, Fe3 and Fe4 atoms are labeled the same as in figures 3, 4 and figure 7. For comparison the results for the free Fe_4 cluster are also listed. (Notice that the data listed below were obtained directly from Mulliken population analysis, and may contain certain errors owing to the method limits.)

		Fe1			Fe2			Fe3			Fe4		
		s	p	d	s	p	d	s	p	d	s	p	d
Free Fe_4	q	0.33	0.94	6.73	0.33	0.94	6.73	0.33	0.94	6.73	0.33	0.94	6.73
	μ_{Fe}	0.21	0.16	3.13	0.21	0.16	3.13	0.21	0.16	3.13	0.21	0.16	3.13
(5, 5)T1	q	0.70	0.53	6.77	0.64	0.56	6.83	0.64	0.59	6.81	0.64	0.59	6.80
	μ_{Fe}	−0.01	−0.01	2.95	−0.01	−0.01	2.74	0.01	0.00	2.93	0.01	0.00	2.92
(5, 5)T2	q	0.66	0.55	6.82	0.68	0.51	6.81	0.63	0.59	6.81	0.63	0.59	6.80
	μ_{Fe}	−0.01	−0.01	2.86	0.00	0.00	2.90	0.01	−0.01	2.97	0.01	−0.01	2.92
(6, 6)T1	q	0.73	0.45	6.78	0.59	0.57	6.86	0.73	0.45	6.78	0.59	0.57	6.86
	μ_{Fe}	−0.01	0.00	3.02	0.01	−0.01	2.76	−0.01	0.00	3.02	0.01	−0.01	2.76
(6, 6)T2	q	0.62	0.55	6.86	0.61	0.56	6.94	0.62	0.55	6.86	0.98	0.23	6.73
	μ_{Fe}	0.03	0.01	2.75	−0.03	−0.01	2.26	0.03	0.01	2.74	0.04	0.02	3.12
(6, 6)CH	q	0.67	0.51	6.80	0.65	0.55	6.86	0.65	0.55	6.85	0.66	0.51	6.81
	μ_{Fe}	0.08	0.02	2.96	0.01	−0.01	2.62	0.01	−0.01	2.63	0.08	0.03	2.96
(8, 0)T	q	0.63	0.62	6.82	0.61	0.61	6.83	0.64	0.62	6.79	0.67	0.59	6.77
	μ_{Fe}	0.02	0.01	2.70	0.03	0.00	2.71	0.03	0.01	2.88	0.05	0.02	3.02

with C states, have received electrons from carbon with the exceptions of Fe1 and Fe4 in the (6, 6)CH structure. The largest charge transfer occurs for the Fe2 in (6, 6)T2 with an extra charge of 0.11 e. As seen below in table 3, the extra electrons fill the 3d states of Fe atom and decrease its spin polarization.

For more details, we calculate the orbital-projected charge and spin polarization for the Fe atoms in confined Fe_4 clusters by Mulliken population analysis and compare them with the results for free Fe_4 in table 3. Compared with the free Fe_4 cluster, the s and p spin polarizations of Fe atoms in all the confined Fe_4 clusters are suppressed owing to the Fe–C sp hybridization, which leads to an overall reduction of the μ_{Fe} by about 0.4 μ_B. Moreover, we find a charge transfer from sp to d with an amount of about 0.05–0.1 e. Together with the electrons from C atoms, the extra electrons filled in Fe 3d states decrease the μ_{Fe} further.

To address the influence of Fe–C hybridization on the magnetic moments of the confined Fe_4 in CNTs, we compare in figure 6 the orbital-resolved local DOS calculated for two Fe atoms with extremely different environments, Fe2 and Fe4 in the (6, 6)T2 structure. As mentioned above, Fe2 has the strongest interaction with the C atoms located in a C–C hexagon while Fe4 away from the tube wall experiences no direct interaction with carbon. Compared to the Fe4, the Fe2 DOS exhibits a more extended structure, signaling stronger hybridization. The weaker sp states for Fe2 indicate a prominent charge transfer to 3d. Looking at the 3d states, we find a larger spin splitting for the Fe4, where the spin-up states lie below and the spin-down states above those of Fe2.

Finally, we have investigated the Fe_4 cluster confined in the semiconducting (8, 0) tube to compare with the results of metallic tubes. We only find one stable Fe_4 cluster configuration with ferromagnetic ground state in the (8, 0) tube. The optimized structure and DOS are shown in figure 7. The four Fe atoms prefer the top site on a C atom in the (8, 0) tube to the top site

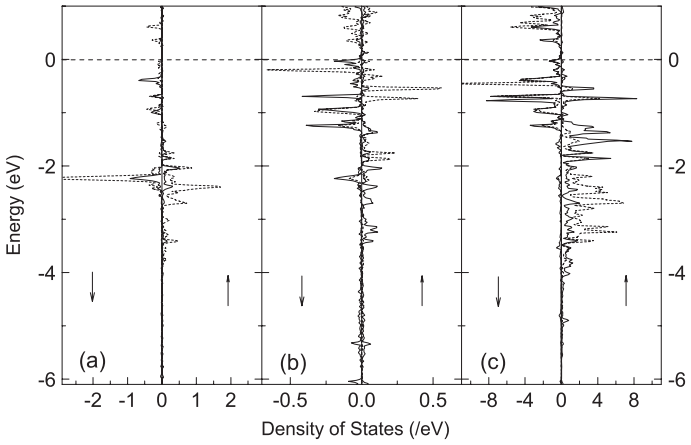

Figure 6. Spin-polarized local DOS for the Fe2 (solid line) and the Fe4 (dashed line) atoms in $Fe_4 + (6, 6)$ with the (6, 6)T2 structure. Shown in panels (a), (b) and (c) are the s-, p- and d-projected DOSs, respectively. The Fermi energy is set to 0.0 eV. The arrows indicate majority (up) and minority (down) spins.

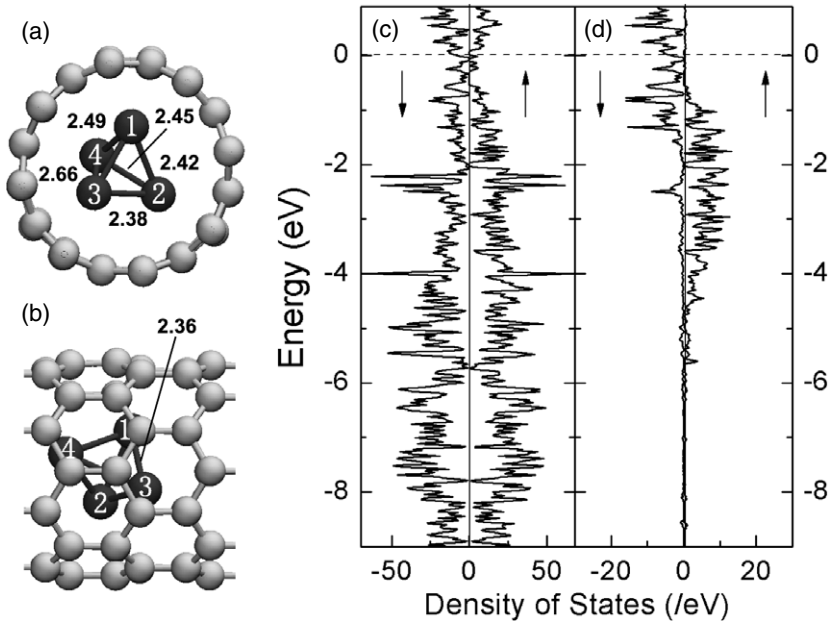

Figure 7. (a) Top and (b) side views of the optimized tetrahedral (8, 0)T structure. The Fe–Fe bond lengths are also shown in the figures (unit: Å). (c) The total DOS and (d) partial DOS for the confined Fe_4 clusters of the (8, 0)T systems. The Fermi energy is set to 0.0 eV. The arrows indicate majority (up) and minority (down) spins.

of a C–C hexagonal center in (5, 5) and (6, 6) tubes, which should be due to different periodic potentials ('templating' effect) between the armchair and zigzag CNTs. This proves a possible method to control the structure of atomic size clusters by the periodic potentials of CNTs. Because the (8, 0) tube has similar diameter to the (5, 5) tube, the binding energies are closer, 4.31 eV for (8, 0)T and 4.85 eV for (5, 5)T2 as listed in table 1. Both of them are about 1 eV

higher than for the (6, 6) tube, which suggests that the binding energy depends on the curvature of the CNTs. In tables 1 and 2 and figures 7(c), (d), the spin moment of the Fe_4 cluster and electronic structures of (8, 0)T are also similar to (5, 5)T2 and (6, 6)T2. We consider that a new Fermi level forms in Fe_4 + CNTs compounds when the Fe_4 clusters combine with CNTs, so the electronic structures near the Fermi level in pristine CNTs do not play an important role in the whole compound.

4. Conclusion

We have investigated the Fe_4 cluster confined in single-walled (5, 5), (6, 6) and (8, 0) CNTs by first-principles calculations. The competition of the existing Fe–Fe bonds with the 'templating' effect of CNTs owing to its periodic axial and circumferential potentials distorts the D_{2d} structure of the Fe_4 cluster, and results in various stable Fe_4 structures confined in the CNTs. Compared with the compact tetrahedral structures in the smaller (5, 5) tube, the Fe_4 confined in the (6, 6) tube demonstrate more flexibility in structure and magnetic properties. In zigzag (8, 0) CNTs, Fe atoms prefer the top site on a C atom in an (8, 0) tube to the top site of a C–C hexagonal center in (5, 5) and (6, 6) tubes, which must be due to different periodic potentials between the armchair and zigzag CNTs.

We further find that strong Fe–C hybridization in confined Fe_4 + CNT structure suppresses the sp spin polarization of Fe atoms and induces prominent change transfer from sp to Fe 3d states, both of which reduce the magnetic moments of the Fe atoms dramatically. However, Fe atoms in the 'Fe4 + CNT' compound still keep higher spin polarization than bulk iron. This compound should be a potential spin-polarized nano-material for its chemical stability and easy manipulation. As the first step of our broad interest in metal clusters interacting with CNTs, our study suggested that the carbon nanotube could be further exploited as a template or regulator for the design of nanoscale magnets with controllable properties.

Acknowledgment

S Yuan acknowledges the financial and computational support from Max-Planck-Gesellschaft.

References

[1] Robertson J 2004 *Mater. Today* **7** 46
[2] Tans S J, Devoret M H, Dai H, Thess A, Smalley R E, Geerligs L J and Dekker C 1997 *Nature* **386** 474
[3] Rueckes T, Kim K, Joselevich E, Tseng G Y, Cheung C-L and Lieber C M 2000 *Science* **289** 94
[4] Bachtold A, Hadley P, Nakanishi T and Dekker C 2001 *Science* **294** 1317
[5] Fennimore A M, Yuzvinsky T D, Han W-Q, Fuhrer M S, Cumings J and Zettl A 2003 *Nature* **424** 408
[6] Terrones M, Hsu W K, Schilder A, Terrones H, Grobert N, Hare1 J P, Zhu Y Q, Schwoerer M, Prassides K, Kroto H W and Walton D R M 1998 *Appl. Phys.* A **66** 307
[7] Hummer G, Rasalah J C and Noworyta J P 2001 *Nature* **414** 188
[8] Khlobystov A N, Britz D A, Andrew G and Briggs D 2005 *Acc. Chem. Res.* **38** 901
[9] Kim B M, Qian S and Bau H H 2005 *Nano Lett.* **5** 873
[10] Hu J, Bando Y, Zhan J, Zhi C and Golberg D 2006 *Nano Lett.* **6** 1136
[11] Su Y-C and Hsu W-K 2005 *Appl. Phys. Lett.* **87** 233112
[12] Fujita T, Hayashi Y, Tokunaga T and Yamamoto K 2006 *Appl. Phys. Lett.* **88** 243118
[13] Korneva G, Ye H, Gogotsi Y, Halverson D, Friedman G, Bradley J-C and Kornev K G 2005 *Nano Lett.* **5** 879
[14] Elias A L, Rodriguez-Manzo J A, McCartney M R, Golberg D, Zamudio A, Baltazar S E, Lopez-Urias F, Munoz-Sandoval E, Gu L, Tang C C, Smith D J, Bando Y, Terrones H and Terrones M 2005 *Nano Lett.* **5** 467
[15] Yang C-K, Zhao J and Lu J P 2003 *Phys. Rev. Lett.* **90** 257203
[16] Yagi Y, Briere T M, Sluiter M H F, Kumar V, Farajian A A and Kawazoe Y 2004 *Phys. Rev.* B **69** 075414

[17] Lee Y-H, Kim D H, Kim D H and Ju B-K 2006 *Appl. Phys. Lett.* **89** 083113
[18] Fagan S B, Mota R, da Silva A J R and Fazzio A 2003 *Phys. Rev.* B **67** 205414
[19] Kang Y-J, Choi J, Moon C-Y and Chang K J 2005 *Phys. Rev.* B **71** 115441
[20] Weissmann M, García G, Kiwi M, Ramírez R and Fu C-C 2006 *Phys. Rev.* B **73** 125435
[21] Jin-Phillipp N Y and Rühle M 2004 *Phys. Rev.* B **70** 245421
[22] Peng D L, Zhao X, Inoue S, Ando Y and Sumiyama K 2004 *J. Magn. Magn. Mater.* **292** 143
[23] Ordejón P, Artacho E and Soler J M 1996 *Phys. Rev.* B **53** R10441
Soler J M, Artacho E, Gale J D, Garca A, Junquera J, Ordejón P and Sánchez-Portal D 2002 *J. Phys.: Condens. Matter* **14** 2745
Soler J M, Beltran M R, Michaelian K, Garzon I L, Ordejón P, Sánchez-Portal D and Artacho E 2000 *Phys. Rev.* B **61** 5771
[24] Troullier N and Martins J L 1991 *Phys. Rev.* B **43** 1993
[25] Kleinman L and Bylander D M 1982 *Phys. Rev. Lett.* **48** 1425
[26] Anglada E, Soler J M, Junquera J and Artacho E 2002 *Phys. Rev.* B **66** 205101
[27] García-Suárez V M, Newman C M, Lambert C J, Pruneda J M and Ferrer J 2004 *J. Phys.: Condens. Matter* **16** 5453
[28] Perdew J P, Burke K and Ernzerhof M 1996 *Phys. Rev. Lett.* **77** 3865
[29] Hobbs D, Kresse G and Hafner J 2000 *Phys. Rev.* B **62** 11556
[30] Cox D M, Trevor D J, Whetten R L, Rohlfing E A and Kaldor A 1985 *Phys. Rev.* B **32** 7290
[31] de Heer W A, Milani P and Chatelain A 1990 *Phys. Rev. Lett.* **65** 488
[32] Billas I M L, Becker J A, Chatelain A and de Heer W A 1993 *Phys. Rev. Lett.* **71** 4067
[33] Billas I M L, Chatelain A and de Heer W A 1994 *Science* **265** 1682
[34] Oda T, Pasquarello A and Car R 1998 *Phys. Rev. Lett.* **80** 3622
[35] Diéguez O, Alemany M M G, Rey C, Ordejón P and Gallego L J 2001 *Phys. Rev.* B **63** 205407
[36] Bobadova-Parvanova P, Jackson K A, Srinivas S, Horoi M, Koehler C and Seifert G 2002 *J. Chem. Phys.* **116** 3576